

Optical Engineering

OpticalEngineering.SPIEDigitalLibrary.org

Practical method for evaluating optical image defects caused by center artifacts

Takao Tanabe
Masato Shibuya
Kazuhisa Maehara

Practical method for evaluating optical image defects caused by center artifacts

Takao Tanabe,^{a,b,*} Masato Shibuya,^a and Kazuhisa Maehara^a

^aTokyo Polytechnic University, Iiyama, Faculty of Engineering, Atsugi, Kanagawa, Japan

^bShowa Optronics Co., Ltd., Engineering Division, Hakusan, Midoriku, Yokohama, Kanagawa, Japan

Abstract. In modern optical element manufacturing, center artifacts are a common problem. A center artifact is a shape error that is rotationally symmetrical, steep, and localized at the center. These properties cause characteristic image defects different from those caused by ordinary irregularities. However, tolerancing center artifacts has not been fully discussed or properly carried out. We propose a simple mathematical model for center artifacts using normal distribution function as a figure model and showing that this function can be represented by a polynomial including odd-order terms. Our method enables appropriate optical simulation and tolerancing for center artifacts using general optical design software. © The Authors. Published by SPIE under a Creative Commons Attribution 3.0 Unported License. Distribution or reproduction of this work in whole or in part requires full attribution of the original publication, including its DOI. [DOI: [10.1117/1.OE.56.8.085103](https://doi.org/10.1117/1.OE.56.8.085103)]

Keywords: center artifacts; irregularities; normal distribution; odd-order aspherical surface; tolerancing.

Paper 170715 received May 11, 2017; accepted for publication Jul. 27, 2017; published online Aug. 21, 2017.

1 Introduction

Optical elements such as lenses, mirrors, and prisms are traditionally fabricated by grinding, smoothing, and polishing.¹ Recently, point processing methods, such as precision turning and magnetorheological finishing have become widely used.^{1–6} The former is mainly applied to generate aspherical profiles on soft materials, such as plastics⁴ and infrared materials.^{4–6} The latter is widely applied to precision finishing or when introducing small asphericity to optical surfaces.

One of the common problems with these point finishing methods is center artifacts⁷ (this is also called “center error”^{8,9}). Center artifacts are rotationally invariant figure errors and localized at the center of optical surfaces. The typical interferometric image is shown in Fig. 14 of Ref. 8, Fig. 2.3 of Ref. 9, and page 13 of Ref. 10.

Center artifacts can affect imaging performance of optical systems. As will be described in Sec. 3, the steep figure error of center artifacts in the front group in wide angle lenses seriously affects image performance at the center image field and causes characteristic diffraction rings because the ray fan of the image is narrow in the front group. Even though center artifacts are small in spread size, they can cause serious defects in image quality in this case. Therefore, tolerancing on center artifacts is one of the important issues in optical design and fabrication. Since the influences of center artifacts have not been fully analyzed, we should properly model their figures for appropriately evaluating tolerance.

In the field of optical design and production, the figure error of optical surfaces from the designed form is generally expressed by the set of Zernike polynomials.¹¹ This set of polynomials was first introduced by Zernike¹² and there are many ways to arrange them.^{11,13,14} Among these, the set of Fringe Zernike polynomials which contains 37 specific terms of circle polynomials^{15,16} is commonly utilized. One of the practical examples is expressed in Ref. 17 by the

use of Grid Sag and Fringe Zernike Surfaces in Zemax. The components of figure error that cannot be expressed by the Fringe Zernike polynomials are classified as midspatial frequency errors, which are considered as somewhat random.^{18,19} However, center artifacts are never expressed by Fringe Zernike expansion and can hardly be evaluated by midspatial frequency error because their peak-to-valley (PV) is large relative to that of midspatial frequency.

To date, the image defects that are caused by center artifacts have not been sufficiently discussed and evaluated. We have investigated this issue and provided a new method for expressing the shape of center artifacts in this paper.

First, we investigated a new mathematical expression of center artifacts. We infer that the normal distribution function provides a close approximation of center artifacts because the normal distribution function is bell shaped. Also since the normal distribution function is characterized by its width and height, the tolerance of the drawing is simple and can be easily understood for manufacturing. Before approximating by the normal distribution function, we employ Zernike fitting to remove figure errors of lower frequencies. Since the normal distribution function is not available in most optical software, it is necessary to rewrite it as a polynomial. However, doing this by using an even-order aspherical surface is not suitable for two reasons: one is that the Taylor expansion of the normal distribution function does not provide a suitable approximation function with any practical finite number of terms. The other is that Fringe Zernike expansion of the normal distribution function provides insufficient approximation for steep normal distribution.

Next, we constructed a method for describing steep normal distribution by utilizing odd-order surfaces. In our investigations of the characteristics of odd-order surfaces,^{20,21} we have analogically predicted that steep normal distribution can be sufficiently represented by a small finite number of power terms including odd-order terms which can be used in many kinds of optical design software. Actually,

*Address all correspondence to: Takao Tanabe, E-mail: t-tanabe@soc-ltd.co.jp

we confirmed the fulfillment of this prediction numerically. Therefore, we could properly express the center artifacts by a small finite number of power terms including odd-order terms. Thus using commercial optical software, we could numerically calculate the changes in point-spread-function (PSF) and modulation transfer function (MTF) caused by center artifacts. Hence, our evaluation method for center artifacts is effective in optical design and development.

2 Mathematical Expressions for Center Artifact

2.1 Impossibility of Expressing Center Artifacts by Fringe Zernike Polynomials

In optical element manufacturing, it is common to describe manufacturing errors using Fringe Zernike polynomials. Reference 16 represents some practical methods for representing irregular surfaces by the use of Zernike polynomials. However, it is impossible to express center artifacts this way. One reason is that the width of a low Zernike polynomial, such as Z_9 is too wide to express steep center artifacts. Another reason is that higher Zernike polynomials, such as Z_{16} , Z_{25} , Z_{36} , and Z_{37} have ripples at the outer region of the aperture. To numerically prove this, let us take a precision turned plastic lens as an example as follows.

The surface deviation is measured using UA-3P, a three dimensional measurement system along two perpendicular directions on the lens surface. Since these two profiles do not differ largely from each other, the surface profile can be approximated as rotationally invariant. Figure 1 shows one direction, in which the horizontal axis is the normalized radial coordinate and the vertical axis is the deviation in millimeters. The marginal coordinate corresponds to 26-mm diameter in exact scale. The blue line describes surface profile in one direction and the red line its approximation represented by the rotationally invariant Fringe Zernike polynomials ($Z_1, Z_4, Z_9, Z_{16}, Z_{25}, Z_{36}$, and Z_{37}). Figure 2 represents the difference between the two lines. Although Zernike fitting can provide an approximation for lower frequency errors, it is completely insufficient to express the center artifact. Therefore, we needed to construct a new mathematical method to express center artifacts.

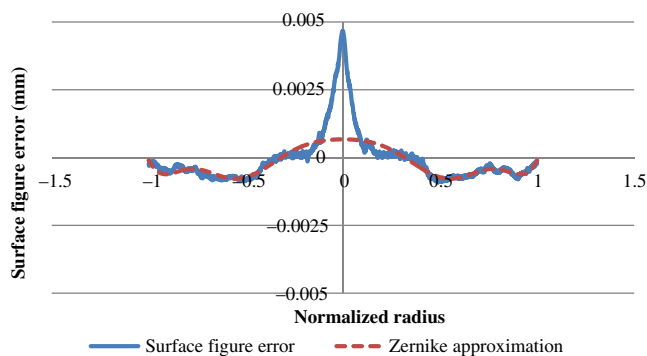


Fig. 1 An example of surface figure error and its Zernike approximation.

2.2 Approximation of Center Artifacts by Normal Distribution Function

As seen in Sec. 2.1, so as to express the shape of center artifacts mathematically, we should introduce another mathematical representation other than Zernike polynomials. Since center artifacts are sharply convex shaped localized at the center, they can be represented by the normal distribution function. Equation (1) can provide a simple mathematical model for representing a center artifact.

$$f(r) = A \exp\left(-\frac{r^2}{\sigma^2}\right). \quad (1)$$

In this mathematical model, the maximum is A , the minimum is 0, and full width at half maximum (FWHM) of $f(r)$ is 2.53σ . We do not need the DC component in Eq. (1), because it is automatically considered by Zernike polynomials fitting. When σ becomes smaller, the profile of the center profile becomes steeper. In the case of Fig. 2, we decided $A = 0.0036$, $\sigma = 0.0546$ by least square method. Figure 3 compares the Zernike fitting error and the mathematical model described in Eq. (1).

Figure 4 shows the residual of figure error. This figure represents that the use of normal distribution approximates the center artifact profile with submicron accuracy, which is satisfactory for precision turned plastic lenses. Therefore, we concluded that it is suitable to express the shape of the center artifact by the use of the normal distribution function. Also since the normal distribution function is characterized by its width and height, the tolerance of the drawing is simple and can be easily understood for manufacturing.

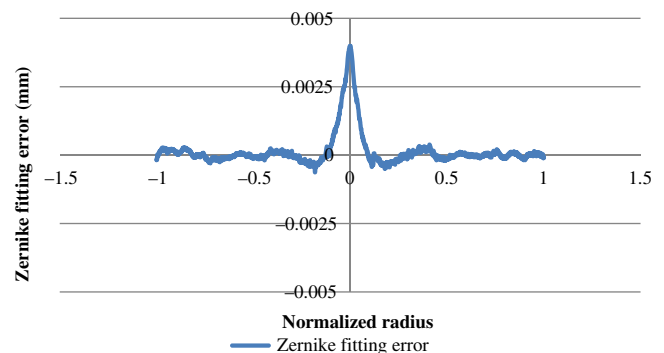


Fig. 2 Fitting error of center artifact using 12th-order Fringe Zernike polynomials.

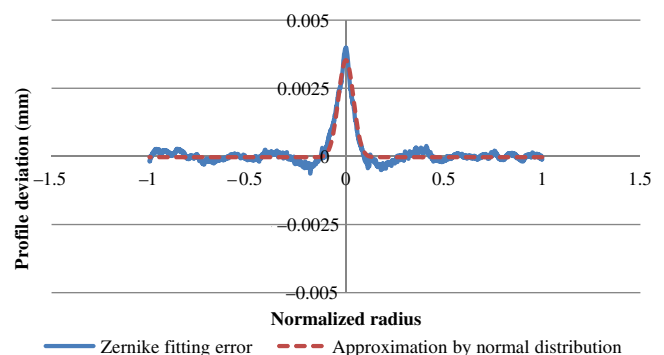


Fig. 3 Zernike fitting error and its approximation by Eq. (1).

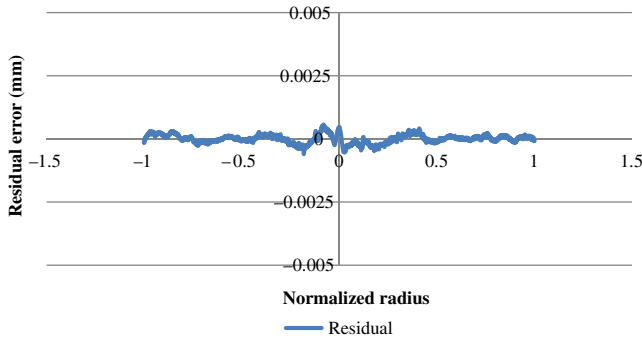


Fig. 4 The residual of an approximation using normal distribution function.

2.3 Impossibility of Expressing the Normal Distribution Function by Even-Order Aspherical Surfaces

Section 2.2 represents the possibility of expressing center artifacts using the normal distribution function. However, since the normal distribution function is generally not prepared in ordinary optical design software, we should rewrite Eq. (1) as the general form for aspherical surfaces.

In Secs. 2.3.1 and 2.3.2, we will discuss the expression of normal distribution by the use of even-order surfaces, the most popular surface type in optical design. Subsection 2.3.1 employs Taylor expansion of normal distribution and Sec. 2.3.2 employs Zernike expansion. We will show that these two methods do not provide sufficient approximation for the normal distribution.

2.3.1 Approximation by Taylor expansion

First, we considered Taylor expansion, which is the most direct method to obtain polynomials. Equation (2) represents the result of expanding $\exp(-r^2/\sigma^2)$ to the power series of r .

$$\exp\left(-\frac{r^2}{\sigma^2}\right) \sim 1 - \frac{r^2}{\sigma^2} + \frac{1}{2} \frac{r^4}{\sigma^4} - \frac{1}{6} \frac{r^6}{\sigma^6} + \dots + \frac{(-1)^n}{n!} \left(\frac{r^2}{\sigma^2}\right)^n + \dots \quad (2)$$

However, the power series of Eq. (2) does not provide suitable approximation using any finite number of terms. Figure 5 compares the power series up to 30th (the upper limit of ordinary even-order aspherical surface in code-V™)

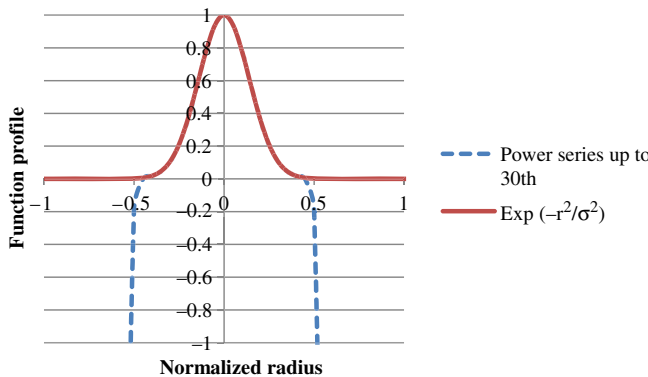


Fig. 5 Comparison of the power series up to 30th with the normal distribution function for $\sigma = 0.2$.

with the original normal distribution function $\exp(-\frac{r^2}{\sigma^2})$ for $\sigma = 0.2$. Figure 5 represents that the power series is an accurate approximation for $r < 0.5$, however, it diverges over the outer area, providing that this power series is not valid for expressing center artifact shape.

2.3.2 Approximation by Zernike expansion

Next, we considered Zernike expansion for the normal distribution function. The example of a center artifact described in Sec. 2.1 cannot be approximated by Fringe Zernike polynomials. However since Zernike polynomials are complete, the normal distribution function can be expressed using a sum of Zernike polynomials.

Equation (3) describes rotationally invariant Zernike polynomials²⁰

$$Q_n(t) = \frac{(-1)^n}{n!} \frac{d^n}{dt^n} t^n (1-t)^n, \quad (3)$$

where t is the square of the radial coordinate r . Table 1 represents the relationship between Eq. (3) and Fringe Zernike polynomials

Fringe Zernike expansion of function $f(t)$ is

$$f(t) = c_0 Q_0(t) + c_1 Q_1(t) + c_2 Q_2(t) + c_3 Q_3(t) + c_4 Q_4(t) + c_5 Q_5(t) + c_6 Q_6(t), \quad (4)$$

where c_n 's are Fringe Zernike coefficients which are calculated by

$$c_n = (2n + 1) \int_0^1 f(t) Q_n(t) dt. \quad (5)$$

Note that Fringe Zernike polynomials satisfy orthogonality, but the ordinary normalization is not satisfied.

To estimate the accuracy of Fringe Zernike expansion of center artifacts, we calculated Fringe Zernike coefficients c_n for the normal distribution function $\exp(-r^2/\sigma^2)$. Equations (4) and (5) lead to Eq. (6) and Table 2 represents the numerical result

Table 1 Relationship between $Q_n(t)$ of Eq. (3) and Fringe Zernike polynomials.

Definition in Eq. (3)	Fringe Zernike	Description
$Q_0(t)$	Z_1	1
$Q_1(t)$	Z_4	$2r^2 - 1$
$Q_2(t)$	Z_9	$6r^4 - 6r^2 + 1$
$Q_3(t)$	Z_{16}	$20r^6 - 30r^4 + 12r^2 - 1$
$Q_4(t)$	Z_{25}	$70r^8 - 140r^6 + 90r^4 - 20r^2 + 1$
$Q_5(t)$	Z_{36}	$252r^{10} - 630r^8 + 560r^6 - 210r^4 + 30r^2 - 1$
$Q_6(t)$	Z_{37}	$924r^{12} - 2772r^{10} + 3150r^8 - 1680r^6 + 420r^4 - 42r^2 + 1$

Table 2 Fringe Zernike coefficients of $\exp(-r^2/\sigma^2)$.

n	c_n
0	$\sigma^2(1 - e^{-1/\sigma^2})$
1	$6\sigma^4(1 - e^{-1/\sigma^2}) - 3\sigma^2(1 + e^{-1/\sigma^2})$
2	$(60\sigma^6 + 5\sigma^2)(1 - e^{-1/\sigma^2}) - 30\sigma^4(1 + e^{-1/\sigma^2})$
3	$(840\sigma^8 + 84\sigma^4)(1 - e^{-1/\sigma^2}) - (420\sigma^6 + 7\sigma^2)(1 + e^{-1/\sigma^2})$
4	$(15120\sigma^{10} + 1620\sigma^6 + 9\sigma^2)(1 - e^{-1/\sigma^2}) - (7560\sigma^8 + 180\sigma^4)(1 + e^{-1/\sigma^2})$
5	$(332640\sigma^{12} + 36960\sigma^8 + 330\sigma^4)(1 - e^{-1/\sigma^2}) - (166320\sigma^{10} + 4620\sigma^6 + 11\sigma^2)(1 + e^{-1/\sigma^2})$
6	$(8648640\sigma^{14} + 982800\sigma^{10} + 10920\sigma^6 + 13\sigma^2)(1 - e^{-1/\sigma^2}) - (4324320\sigma^{12} + 131040\sigma^8 + 546\sigma^4)(1 + e^{-1/\sigma^2})$

$$c_n = (-1)^n \frac{(2n+1)}{n!} \int_0^1 \exp(-t/\sigma^2) \frac{d^n}{dt^n} t^n (1-t)^n dt. \quad (6)$$

Figure 6 compares normal distribution functions for $\sigma = 0.2, 0.1, 0.05$ with their Fringe Zernike expansion and Table 3 lists the coefficients explicitly. Figure 6 explains that the Fringe expansion of the normal distribution function for small σ is insufficient to approximate the original functions even if all terms up to the 37th (upper limit of Fringe Zernike polynomials) are used. Thus, the set of Fringe Zernike polynomials is inappropriate to express the shape of the normal distribution function.

The discussion in Secs. 2.2, 2.3.1, and 2.3.2 leads to the conclusion that the shape of a steep center artifact can be expressed by neither finite number even-order terms nor by Fringe Zernike expansion.

2.4 Expressing the Normal Distribution Function by Power Terms Including Odd-Order

Since we proved that the normal distribution function is not represented by even-order aspherical surfaces in Sec. 2.3, we introduced odd-order aspherical surface in order to express center artifact. According to our investigations of the characteristics of odd-order surfaces, we have analogically predicted that center artifact shape can be sufficiently represented by a small finite number of power terms including odd-order terms which can be used in most optical design software.

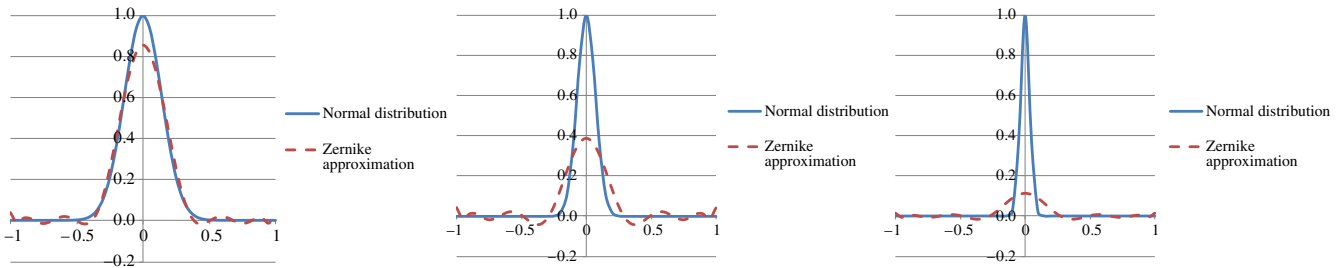


Fig. 6 Comparison of normal distribution functions for $\sigma = 0.2, 0.1, 0.05$ and their Fringe Zernike expansion.

Table 3 Fringe Zernike coefficients for normal distribution function.

Coefficients	σ		
	0.2	0.1	0.05
c_0	0.040000	0.010000	0.002500
c_1	-0.110400	-0.029400	-0.007463
c_2	0.155840	0.047060	0.012313
c_3	-0.170330	-0.062012	-0.016982
c_4	0.157875	0.073546	0.021400
c_5	-0.128731	-0.081267	-0.025508
c_6	0.094161	0.085104	0.029253

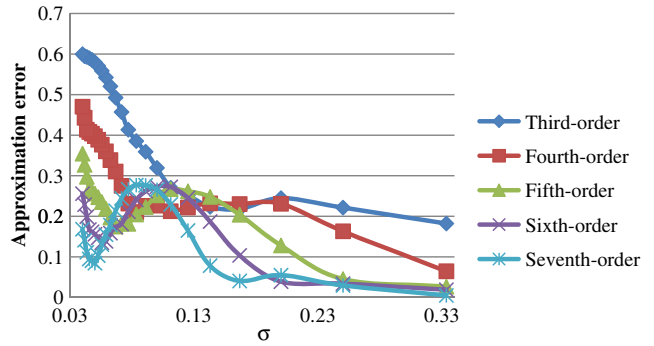


Fig. 7 Maximum approximation error versus σ for Eq. (7).

Equation (7) represents a polynomial of order N including odd-order

$$g(r) = a_0 + a_1|r| + a_2|r|^2 + a_3|r|^3 + \dots + a_N|r|^N. \quad (7)$$

When the curve $z = g(r)$ passes through $N + 1$ points $(r_k, z_k) k = 0, 1, \dots, N$, the coefficients a_k are the solution of the following linear equation:

$$\begin{aligned} a_0 + a_1 r_0 + a_2 r_0^2 + a_3 r_0^3 + \dots + a_N r_0^N &= z_0 \\ a_0 + a_1 r_1 + a_2 r_1^2 + a_3 r_1^3 + \dots + a_N r_1^N &= z_1 \\ &\vdots \\ a_0 + a_1 r_N + a_2 r_N^2 + a_3 r_N^3 + \dots + a_N r_N^N &= z_N. \end{aligned} \quad (8)$$

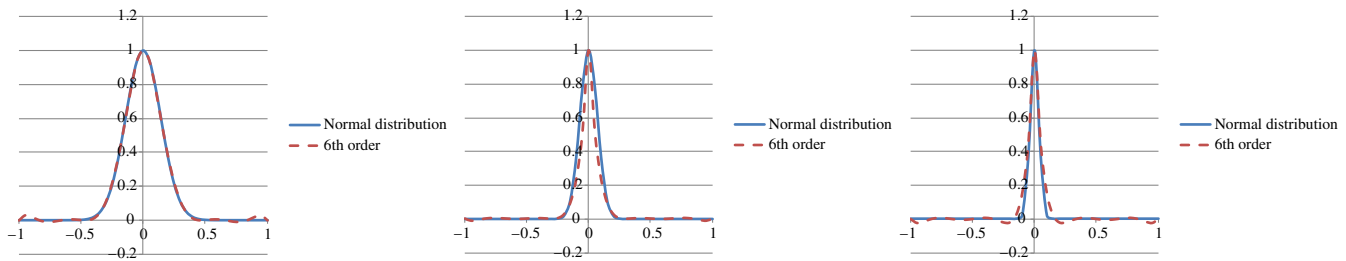


Fig. 8 Approximation curves for $\sigma = 0.2, 0.1,$ and $0.05.$

We considered the function $\exp(-r^2/\sigma^2)$ and choose $N + 1$ points as $(r_k, z_k) = \{\frac{k}{N}, \exp[-(\frac{k}{N})^2/\sigma^2]\}$ at even intervals in the region $r \in [0,1]$. By resolving the linear equation Eq. (8), the coefficients a_k 's were obtained. Figure 7 shows the maximum approximation error curves of Eq. (7) with respect to σ .

Figure 7 explains that the approximation error is nearly saturated when the degree N exceeds 6. In practice, Fig. 8 shows that the normal distribution function can be fully approximated by polynomials of order $N = 6$ for $\sigma = 0.2, 0.1,$ and $0.05.$

The discussion of this section gives an explicit method for approximating center artifacts by polynomials including odd-order.

3 Optical Simulation with Our Proposed Mathematical Model

3.1 Optical Design

Using the new mathematical model we proposed in Sec. 2, we discuss how image quality is affected by center artifacts. For this purpose, we considered a projection lens which is a modified design from Ex. 2 of Ref. 22. The specification is listed in Table 4. Table 5 represents the lens data and Fig. 9 shows the optical configuration of this design. This design consists of eight lenses in which both sides of the second lens are aspherical. Equation (9) is the aspherical description of this design.

$$z = \frac{cr^2}{1 + \sqrt{1 - (1+k)c^2r^2}} + A_2r^2 + A_4r^4 + \dots + A_{12}r^{12}, \tag{9}$$

where c is the curvature, k is the conic constant, r is the (un-normalized) radial coordinate, and A_n are the aspherical coefficients. Aspherical coefficients up to 12th are used in this design.

Table 4 Design specifications for projection optics.

Description	Design specifications
Magnification	71.9×
Effective F number	2.4
Image circle	20-mm diameter
Wavelength	Visible (460 to 630 nm)

Table 5 Lens design data.

Surface	Radius	Thickness	Glass	Conic
OBJ	Infinity	0		
1	Infinity	2000		
2	28	3	S-FSL5	
3	14.71695	5		
4	14.06305	3	PMMA	-0.4915
5	6.768793	20.10655		-1.096
6	44.69331	3.789097	S-LAH51	
7	-68.9588	12		
STO	Infinity	15		
9	1000	2	S-NBH51	
10	21.67184	11	S-FPL51	
11	-14.7272	2	S-LAH63	
12	-29.2365	0.1		
13	65.6066	7.5	S-FPL51	
14	-36.5626	1		
15	68.06173	4	S-TIL26	
16	-1000	7.388574		
17	Infinity	25	S-BSL7	
18	Infinity	3		
19	Infinity	1.05	S-FSL5	
20	Infinity	1.012085		
IMA	Infinity			

Aspherical coefficients:

	Surface 4	Surface 5
A2	0.000000×10^00	0.000000×10^00
A4	$-3.483769 \times 10^{-04}$	$-3.948001 \times 10^{-04}$
A6	2.620559×10^{-06}	4.177955×10^{-06}
A8	$-1.516800 \times 10^{-08}$	$-2.989014 \times 10^{-08}$
A10	4.881588×10^{-11}	1.045121×10^{-10}
A12	$-6.235464 \times 10^{-14}$	$-7.943251 \times 10^{-14}$

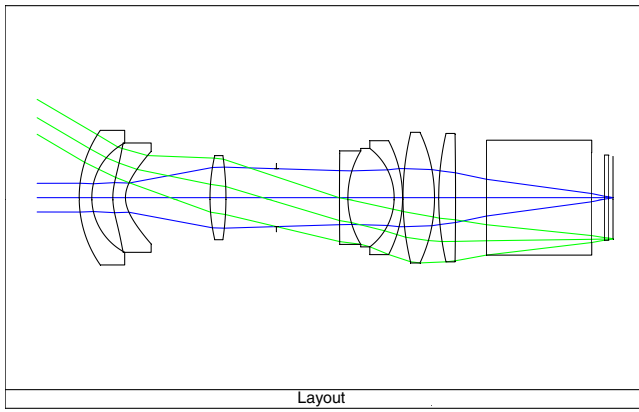


Fig. 9 Optical configuration of the lens represented in Table 4.

Since the size of a pixel for the display device is $10 \mu\text{m}^2$, the Nyquist frequency is 50 lines per millimeters. Thus, Fig. 10 represents the designed MTF curve of this lens in the region, with a maximum frequency twice its Nyquist frequency. The horizontal axis represents spatial frequency and the vertical axis MTF values. As shown in Fig. 10, using aspherical lenses, we obtained excellent optical performance. However, since precision turned plastic lenses sometimes have center artifacts at the lens axis, the image quality of the field center degenerates remarkably in this case. Therefore, the tolerance of PV value and width of center artifacts must be properly obtained.

3.2 Mathematical Representation of Actual Center Artifacts

Aspherical lenses are directly generated from blanks of poly (methyl methacrylate) (PMMA). Figure 11 represents the



Fig. 11 Photograph of the actual turned aspherical lens.

photograph of an actual aspherical lens. Figures 12(a) and 12(b) represent the measured deviation of the manufactured plastic lens from the designed value. Figure 12(a) is the front surface and Fig. 12(b) the rear surface. Table 6 represents the Zernike approximation obtained by direct calculation of inner products of actual surface figure errors and Zernike polynomials.

By removing the component that was expressed by Fringe Zernike polynomials, Fig. 13 represents the approximations of center artifacts using the normal distribution function. The parameters in Eq. (1) for each surface are shown in Table 7. Parameter A represents the height of the center artifact. The parameter σ shows the width of the center artifact and has no dimension since the radial coordinate is normalized. The solution of linear Eq. (8) for each σ provides its aspherical coefficients.

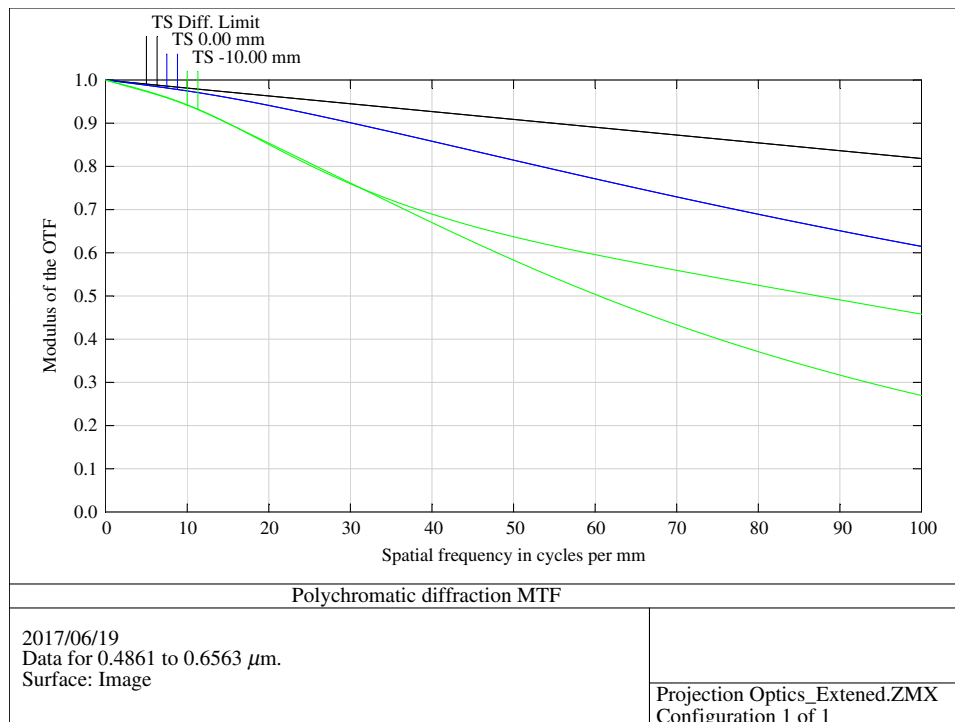


Fig. 10 MTF curve for the design described in Table 4 (blue line: on-axis, green-line: marginal tangential and radial).

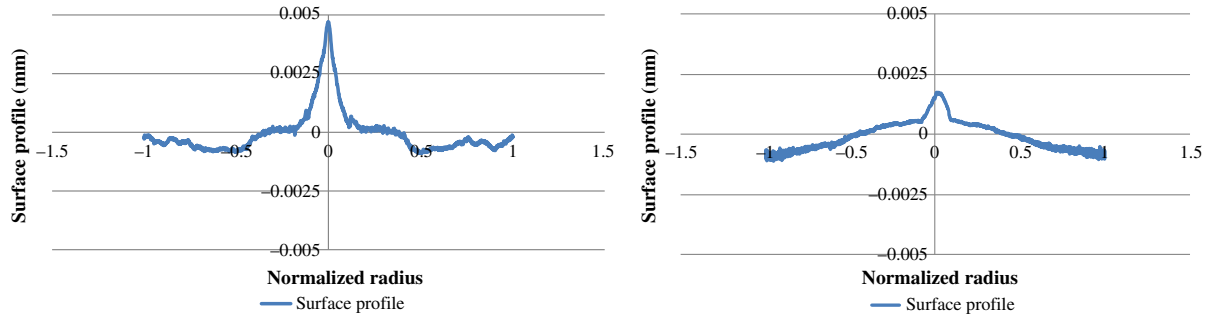


Fig. 12 Measured deviation of the turned lens from the designed shape.

In solving Eq. (8), we normalized $A = 1$ for convenience and Table 7 lists the solutions. Since the coefficients listed in Table 8 are normalized to unify the peak, multiplying actual A (artifact height) to the coefficients provides the actual aspherical coefficients. In addition, when we converted these parameters to match those of an optical simulation program, we had to take care that the polynomial equals the function of the normalized radial coordinate. Figure 14 compares the measured figure errors and the final approximation shapes of center artifacts which contain Fringe Zernike coefficients and odd-order terms.

At the end of this subsection, we discuss the approximation accuracy of the mathematical model for center artifacts. Table 9 shows the PV error of the measured figure and PV residual errors of three approximation methods discussed above.

Table 6 Zernike expansion coefficients of the front and rear surfaces.

	Front surface	Rear surface
c_0	$-4.380795 \times 10^{-04}$	$-4.060442 \times 10^{-04}$
c_1	$-2.054843 \times 10^{-04}$	$-6.654129 \times 10^{-04}$
c_2	4.636624×10^{-04}	3.253009×10^{-04}
c_3	$-3.911798 \times 10^{-04}$	$-1.218029 \times 10^{-04}$
c_4	3.681959×10^{-04}	2.640439×10^{-05}
c_5	2.059885×10^{-04}	$-2.239883 \times 10^{-05}$
c_6	$-1.108508 \times 10^{-04}$	9.774386×10^{-05}

Because of the narrow width of the center artifact in the front surface, Fringe Zernike fitting does not approximate the figure error. Specifically, the Zernike fitting residual of the first surface remains $4.6 \mu\text{m}$ in PV value, which cannot be negligible. However, our new model that employs both Fringe Zernike and normal distribution reduces the residual by 75%. The polynomial model provides almost the same residual as the normal distribution model. Consequently, our mathematical model described in this paper can provide a better description of figure errors that contain center artifacts.

3.3 Optical Simulation

By adding aspherical coefficients for the actual center artifact to the designed lens data, we could evaluate how center artifacts affect the optical performances such as MTF and PSF.

The aspherical surface is represented by Eq. (10):

$$z = \frac{cr^2}{1 + \sqrt{1 - (1+k)c^2r^2}} + \sum_{k=2}^6 A_{2k}r^{2k} + \left\{ \sum_{k=1}^6 c_k Q_k(r^2) + \sum_{k=1}^6 a_k r^k \right\}. \quad (10)$$

In this formula, the first two terms are the original designed form. The additional term, $\{\sum_{k=1}^6 c_k Q_k(r^2) + \sum_{k=1}^6 a_k r^k\}$, represents the figure error. The former $\sum_{k=1}^6 a_k r^k$ is Fringe Zernike components error and the latter $\sum_{k=1}^6 c_k Q_k(r^2)$ is the polynomial representation of center artifacts.

Figure 15 compares the designed MTF, the MTF with Fringe Zernike components error, and the MTF with both

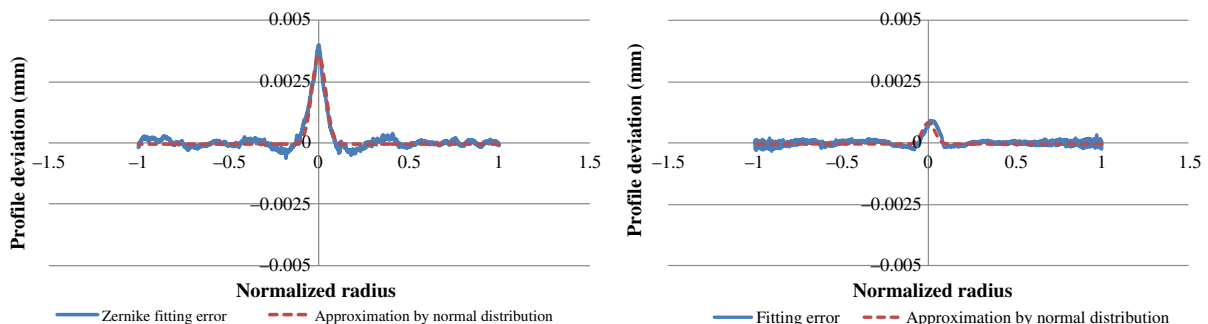


Fig. 13 Approximation of center artifacts using normal distribution function.

Table 7 The parameters of actual fabricated lens for Eq. (1).

Parameter	Front surface	Rear surface
σ (no dimension)	0.0546	0.0508
A (mm)	0.0036	0.0008

Zernike components and center artifacts for the axial image point. Furthermore, Fig. 16 compares the designed PSF, the PSF with Zernike components, and the PSF with both Zernike components and center artifacts. These figures represent that the Zernike components are so small that the values of MTF and PSF remain as high as designed value. On the contrary, the center artifacts obviously affect the PSF. Figure 16(c) shows characteristic diffraction rings around the center, and they affect the imaging quality, such as MTF as shown in Fig. 15(c).

These characteristic diffraction rings and deterioration in MTF are very common in practical lens manufacturing. Hence, the mathematical model of center artifacts can represent the image degeneration of image quality as practical optical systems.

4 Summary

We have proposed an advanced approach to simulate center artifacts shapes for improving image quality by the use of general polynomial forms including odd-order terms. For generating aspherical profiles, precision turning has become common in processing plastics or infrared materials. However, this method can also produce the characteristic shape error called center artifact or “center error.” Center artifacts are rotationally invariant and localized at the center of lens surfaces.

In optical design and manufacturing, surface deviations from designed forms are usually represented by Fringe Zernike polynomials. In addition, components that cannot be represented by Fringe Zernike polynomials are classified as midspatial frequency errors and regarded as random constituents. However, since it is impossible to express center artifacts using Fringe Zernike expansion and they can hardly be evaluated by midspatial frequency errors, the effects of center artifacts have not been properly evaluated, thus tolerancing center artifacts has been next to impossible.

In this paper, we have constructed a practical new method for modeling center artifacts suitable for optical

Table 8 Aspherical coefficients of approximation polynomials.

	Front surface	Rear surface
a_0	1.000000×10^{00}	1.000000×10^{00}
a_1	-1.469677×10^{01}	-1.469924×10^{01}
a_2	8.117187×10^{01}	8.119338×10^{01}
a_3	-2.204062×10^{02}	-2.204779×10^{02}
a_4	3.148497×10^{02}	3.149646×10^{02}
a_5	-2.266836×10^{02}	-2.267726×10^{02}
a_6	6.476508×10^{01}	6.479178×10^{01}

Table 9 P-V errors of measured figure and P-V residuals of three approximation methods (units are in millimeters)

	P-V errors of measured figure	Fringe Zernike approximation residuals	Fringe Zernike and normal distribution residuals	Zernike and odd-order residuals
Front surface	0.0056	0.0046	0.0012	0.0015
Rear surface	0.0029	0.0013	0.0007	0.0009

simulation. We have found that center artifacts can be represented by normal distribution function and this function can sufficiently be expressed by polynomials including odd-order terms. Since ordinary polynomial surfaces are applicable for commercial optical design software, our model can be applied to practical optical design. In our simulation, we have shown that our method provides simple and easy evaluations of center artifacts. In addition, since the shape of the normal distribution function is decided by only standard deviation which corresponds to the width of a bell-shaped curve, this representation provides simple characterization of center artifacts for optical drawing, tolerancing, and fabrication. Through our research, we propose a useful new method for optical design and development.

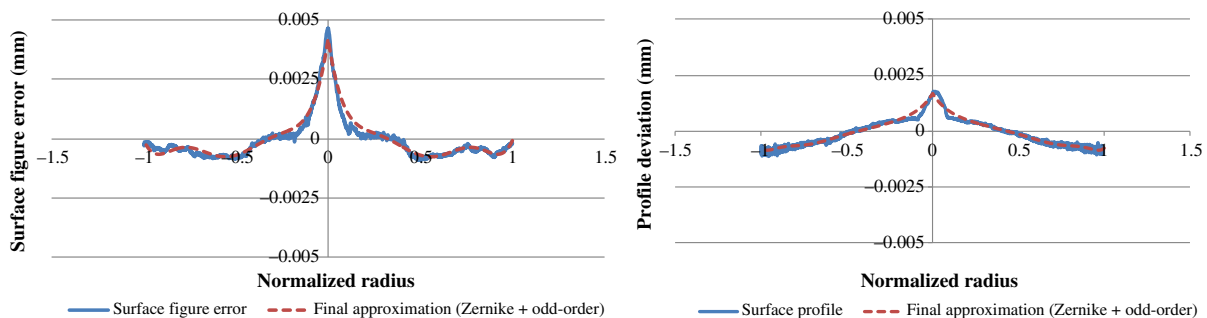


Fig. 14 Measured figure errors and the final approximation shapes.

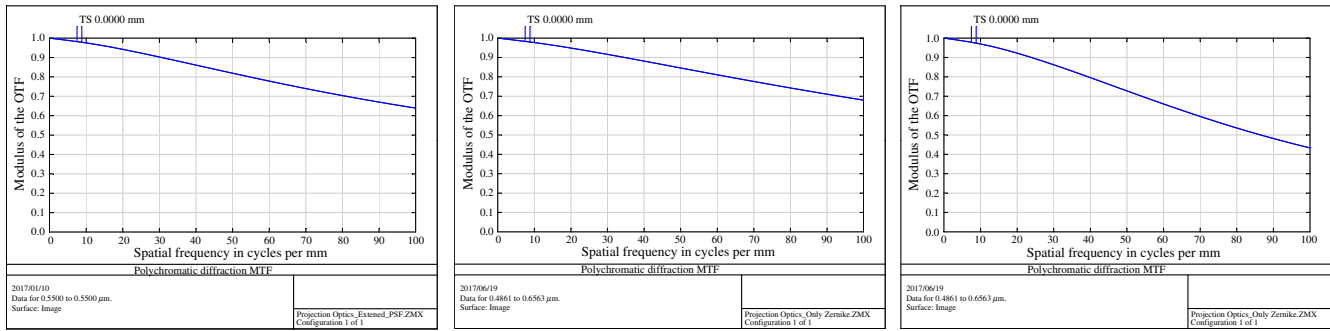


Fig. 15 Comparison of MTF of axial image.

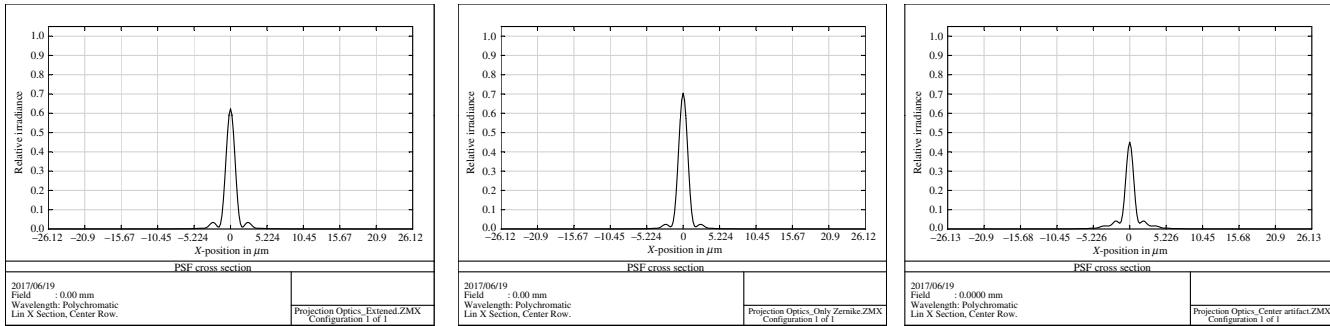


Fig. 16 Comparison of PSF of axial image.

References

1. K. Schwertz, "An introduction to the optics manufacturing process," *OptoMechanics* (OPTI 521) Report (2008).
2. O. Schmelzer and R. Feldkamp, "Precision machining of optical surfaces with subaperture correction technologies MRF and IBF," *Proc. SPIE* **9633**, 96330E (2015).
3. D. Golini et al., "Magneto-rheological finishing (MRF) in commercial precision optics manufacturing," *Proc. SPIE* **3782**, 80 (1998).
4. R. L. Rhorer and C. J. Evans, "Fabrication of optics by diamond turning," Chapter 41 in *Handbook of Optics*, M. Bass et al., Eds., pp. 41.1–41.13, Optical Society of America, Washington (1995).
5. M. J. Dent, "Production aspects of single point diamond turning," *Proc. SPIE* **0508**, 12 (1984).
6. P. M. Parr-Burman and P. Shore, "Diamond turning of silicon optics," *Proc. SPIE* **2775**, 575 (1996).
7. D. C. Harris, "Window and dome technologies and materials," *Proc. SPIE* **8016**, 80160N (2011).
8. J. K. Myler and D. A. Page, "Factors governing surface form accuracy in diamond machined components," *Proc. SPIE* **0915**, 84 (1988).
9. P. R. Hall et al., "Recent achievements in closing the loop in interferometric tool-setting on a pneumo-precision MSG325 diamond turning lathe," *Proc. SPIE* **2576**, 2 (1995).
10. K. K. N. Kogaku, *Through the Lens We Capture the Future*, http://www.eliteoptics100.com/content/images/Nittoh20%Introduction_FINAL.pdf (12 May 2017).
11. D. Malacara et al., *Optical Shop Testing*, 3rd ed., Chapter 13, John Wiley & Sons, Inc., Hoboken (2007).
12. F. Zernike, "Beugungstheorie des schneidenerfahrens und seiner verbesserten form, der phasenkontrastmethode," *Physica* **1**, 689–704 (1934).
13. M. Born and E. Wolf, *Principles of Optics*, 2nd (revised) ed., Cambridge University Press, Cambridge (1999).
14. R. J. Noll, "Zernike polynomials and atmospheric turbulence," *J. Opt. Soc. Am.* **66**(3), 207–211 (1976).
15. Zygo Corporation, *MetroPro Reference Guide OMP-0347K*, pp. 10–30 (August 2006).
16. C. J. Evans, "PVR—a robust amplitude parameter for optical surface specification," *Opt. Eng.* **48**(4), 043605 (2009).
17. R. Melich et al., "Irregular surfaces—measurements and ZEMAX simulations," in *EPJ Web of Conf.*, Vol. **48**, p. 00015 (2013).
18. M. Shibuya et al., "Classification of undulated wavefront aberration in projection optics by considering its physical effects," *Opt. Eng.* **46**(5), 053001 (2007).
19. J. Filherber, "LARGE OPTICS: mid-spatial-frequency errors: the hidden culprit of poor optical performance," *Laser Focus World* **49**, 32 (2013).
20. T. Tanabe et al., "Convergence and differentiation of Zernike expansion: application for an analysis of odd-order surfaces," *Opt. Eng.* **55**(3), 035101 (2016).
21. T. Tanabe and M. Shibuya, "Aberration properties of odd-order surfaces in optical design," *Opt. Eng.* **55**(12), 125107 (2016).
22. Takao Tanabe, Japan Patent Application 250101 (2010).

Takao Tanabe is a lens designer for Showa Optronics Co., Ltd. He received his MS degree in mathematics from Tokyo Institute of Technology in 2005. After an 11-year career at Topcon and 1 year at Hakuto, he transferred to Showa Optronics. He has designed lithographic optics, medical optics, and laser optics. He is studying optics at Tokyo Polytechnic University. He is a professional engineer, Japan (mechanical) and also a member of SPIE.

Masato Shibuya is a professor in the Department of Media and Image Technology, Faculty of Engineering, Tokyo Polytechnic University. He graduated from Tokyo Institute of Technology in 1977 with a master's degree in physics and joined Nikon Corporation. He received his PhD from the University of Tokyo in 1996. He joined Tokyo Polytechnic University in 2001, and his research interests include fundamental lens optics, optical lithography, super-resolution, and phase-shifting mask. He is a SPIE fellow.

Kazuhisa Maehara graduated from the University of Tokyo in 1974 with a master's degree in mathematics and joined the Ministry of Labor. He joined Tokyo Polytechnic University in 1976, and he received his PhD from the University of Tokyo in 1984. He had been an associate professor in Tokyo Polytechnic University until 2011. His research interests include classification of algebraic varieties from the point of view of birational geometry and analytic manifolds. He is also interested in diophantine problems.